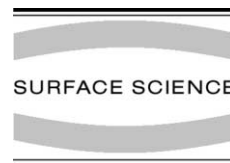




ELSEVIER

Surface Science 507–510 (2002) 124–128



www.elsevier.com/locate/susc

Enhanced iron self-diffusion in the near-surface region investigated by nuclear resonant scattering

M. Sladeczek^{a,*}, B. Sepiol^a, M. Kaisermayr^a, J. Korecki^{b,c}, B. Handke^{b,c},
H. Thies^{a,d}, O. Leupold^d, R. Ruffer^d, G. Vogl^{a,e}

^a *Institut für Materialphysik der Universität Wien, Strudlhofgasse 4, A-1090 Wien, Austria*

^b *Faculty of Physics and Nuclear Techniques, University of Mining and Metallurgy, Mickiewicza 30, PL-30-059 Cracow, Poland*

^c *Institute of Catalysis and Surface Chemistry, PAS, PL-30-239 Cracow, Poland*

^d *ESRF, F-38043 Grenoble, France*

^e *Hahn-Meitner-Institut, D-14109 Berlin, Germany*

Abstract

The access to X-rays of third generation synchrotron radiation sources enables studies of dynamics in metallic systems in grazing incidence geometry. Combining grazing incidence reflection of X-rays with nuclear resonant scattering of synchrotron radiation allows depth-selective investigations of hyperfine parameters and diffusion phenomena of iron and iron compounds. The unique feature of this method is its sensitivity to near-surface motions of atoms and not exclusively to the atoms on the surface. The depth sensitivity can be varied between about two and more than 10 nm. A 300 nm thick ⁵⁷Fe sample grown by molecular beam epitaxy on a cleaved MgO(001) substrate was investigated. The diffusion coefficient of iron in the near-surface layer (thickness about 2 nm) is almost two orders of magnitude larger than in bulk bcc iron at the same temperature. © 2002 Elsevier Science B.V. All rights reserved.

Keywords: Diffusion and migration; Atomistic dynamics; Mössbauer spectroscopy; Molecular beam epitaxy; Iron; Metallic films

1. Introduction

Nuclear resonant scattering (NRS) has become an established technique for studying diffusion on an atomistic scale. The power of the technique was predicted by the theoretical work of Smirnov and Kohn [1,2] and demonstrated by several experiments [3–8]. These works used the technique of nuclear forward scattering and nuclear Bragg scattering which enabled them to investigate the

diffusion mechanism in bulky material. For extending this method to surface sensitivity we have combined the techniques of NRS and grazing incidence reflections, the latter being an established technique in X-ray and neutron scattering for studying the structure and dynamics of thin films.

It has been proven that NRS in grazing incidence geometry provides depth selectivity for hyperfine spectroscopy [9–11]. We will exploit this depth selectivity to investigate diffusion phenomena in near-surface regions of metallic films of iron. Experiments of this kind became feasible with the advent of third generation synchrotron radiation sources.

* Corresponding author. Tel.: +43-1-4277-51332; fax : +43-1-4277-9513.

E-mail address: sladeczek@ap.univie.ac.at (M. Sladeczek).

1.1. Diffusion investigations by nuclear resonant scattering of synchrotron radiation

NRS with synchrotron radiation and Mössbauer spectroscopy are related microscopic techniques for the determination of hyperfine parameters and dynamical properties on an atomistic scale. They measure directly in the time and energy domain, respectively. In NRS the synchrotron radiation pulse creates a coherent collective nuclear state in the sample which may be perturbed or destroyed by diffusion. This leads to an accelerated decay of the resonantly scattered intensity (delayed intensity) with respect to an undisturbed scattering process [1,2]. The delayed intensity is proportional to the intermediate scattering function $I(\mathbf{Q}, t)$ [2] which becomes a simple exponential function in the limit of a thin sample:

$$I(\mathbf{Q}, t) = \exp \left[-\frac{t}{\tau} \sum_{i=1}^N N^{-1} \{1 - \exp(-i\mathbf{Q}\mathbf{l}_i)\} \right], \quad (1)$$

where \mathbf{Q} is the outgoing wave vector, \mathbf{l}_i are jump vectors between lattice sites, τ is the residence time on a lattice site and N is the number of nearest-neighbour lattice sites. The accelerated decay is not only determined by τ but also by the orientation of the crystal axes and the jump vector, respectively, relative to the outgoing wave vector \mathbf{Q} .

1.2. Iron on MgO(001)

For a first feasibility study we have chosen a ^{57}Fe layer on a (001)-MgO substrate. The advantages are as follows:

- The growing mode (layer by layer), the structure of Fe on MgO (bcc), the influence of the MgO substrate on the iron structure and the surface relaxation in the first one up to three layers are well known [12–15].
- The surface of this sample grown by molecular beam epitaxy (MBE) is well defined also at higher temperatures.
- The system is simple, it consists only of iron atoms which give the best performance in NRS studies. Parasitic effects like sample decomposi-

tion, alloying or segregation cannot take place and the measured delayed intensity is high.

- The atomic jump diffusion process in bulk iron is well studied and accepted to be a NN-jump process [16].

2. Experimental

2.1. Sample preparation

The sample was grown by MBE and characterised in situ by low energy electron diffraction and Auger electron spectroscopy under UHV conditions. Detailed preparation conditions and sample characterisation techniques are published earlier [17]. The substrate was a MgO(001) polished single crystal. The iron grows with the [001] normal direction parallel to the [001] one of the MgO substrate. The small lattice mismatch along the [110] direction of MgO (a_{MgO} (RT) = 4.211 Å) with lattices of bcc-Fe(001) (a_{Fe} (RT) = 2.866 Å) causes a 45° rotation of the iron unit cell relative to the MgO cell. The experimentally determined thickness during the MBE growth was 300 nm. The evaluation of the Kiessig X-ray reflectivity beats of synchrotron radiation yielded an iron layer thickness of 270 nm. Additional investigations were done by conversion electron Mössbauer spectroscopy (CEMS) showing the typical value of the magnetic hyperfine field in α -iron.

2.2. Experimental set-up

The measurements were performed at the nuclear resonance station ID22N at the ESRF. The synchrotron radiation was monochromized to an energy bandwidth of 6 meV and focussed vertically to 120 μm . The storage ring was operated in 16 bunch mode providing successive X-ray pulses with 176 ns separation. Avalanche photo diodes with a 100 μm vertical collimator served as fast detectors. Details may be found in Ref. [18].

The sample was measured in a furnace mounted on a goniometer head permitting to orient the sample relative to the synchrotron beam. Special attention was devoted to the determination of the incidence angle of the synchrotron radiation.

An accuracy of about 0.05 mrad was achieved. The zero position was checked after each temperature step.

The furnace with beryllium windows was resistively heated by a Mo wire in a constant-voltage mode. The temperature was stabilized better than 1 K using a thermocouple touching the tantalum sample holder. Below the Curie temperature ($T_c = 1043$ K) the sensor was calibrated against the sample temperature measuring the known temperature dependence of the magnetic hyperfine field in α -iron.

The vacuum was about 10^{-8} mbar, nevertheless, from CEMS measurements no surface oxidation was found after the measurement only a slight distribution of the magnetic field due to mixing of iron and Mg from the substrate. A contamination of the order of 4 at.% Mo from the Mo heater was found by micro-beam fluorescence spectroscopy.

2.3. High temperature measurements

The measurements were performed at an incidence angle of $\theta = 1.66$ mrad. The maximum delayed intensity has been found at an angle $\theta = 3.41$ mrad close to the critical angle of total reflection [9]. However, in order to improve the surface sensitivity the incidence angle of 1.66 mrad was chosen in the presented measurements. Spectra were recorded within the temperature range RT to 1230 K. The paramagnetic spectra above T_c show an accelerated intensity decay due to fast diffusion of the iron atoms. In order to determine the direction of the jump vectors the dependence on the angle ϕ , which is the angle between the in plane iron [1 1 0] direction and the synchrotron radiation beam (Fig. 1), has been measured for values of 38° , 43° , 53° , and 58° .

3. Results

Fits to the delayed intensity spectra were performed using the EFFINO routine written by Spiering et al. [19]. It was impossible to achieve satisfying fits assuming only one iron layer. This model does not describe properly the curvature of the experimental spectrum (see dashed line in Fig. 2

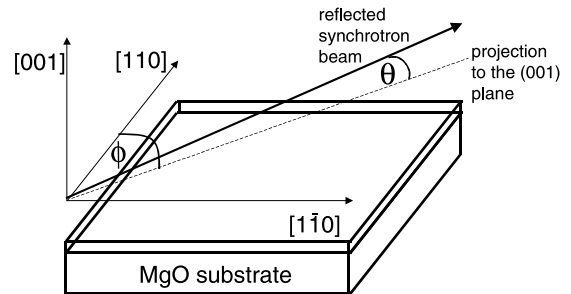


Fig. 1. Sketch of the scattering geometry. θ is the angle of incidence and ϕ is the angle between the [1 1 0] direction of the iron layer and the projection of the outgoing wave vector of the synchrotron radiation to the (0 0 1) plane of the iron layer.

inset). This was achieved using a two-layer model (see Fig. 3 inset). The upper layer is a 2 nm thick near-surface layer with measurable diffusion, the rest is bulk iron without a noticeable diffusion. The attempts to fit the thickness of the near-surface layer led at all three temperatures and for all orientations of the sample to the same value. As shown in Eq. (1) the accelerated intensity decay depends on the relative orientation of the jump

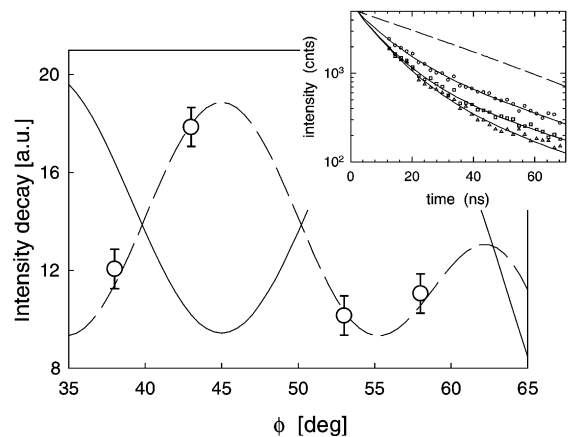


Fig. 2. Angular dependence of the intensity decay at 1200 K and an angle of incidence of $\theta = 1.66$ mrad. The dashed line is calculated for a 2D square-lattice jump diffusion mechanism in the α -iron (001) plane. The solid line is calculated for NN jumps on a bcc lattice in bulk α -iron. The inset shows the delayed intensity for various temperatures (\circ): 1090 K; (\square): 1200 K; (\triangle): 1230 K) and an angle of incidence of $\theta = 1.66$ mrad. The dashed line is an incorrect fit using the single iron layer model.

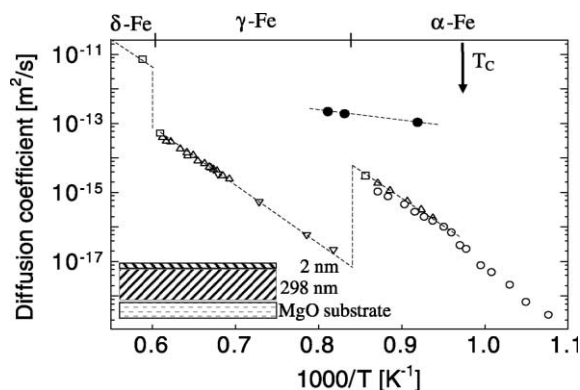


Fig. 3. Comparison of the bulk diffusion coefficient from different tracer measurements (open symbols) [20] and the calculated diffusion coefficient in the near-surface iron layer (full symbols) from measurements at 1090, 1200 and 1230 K, an angle of incidence of $\theta = 1.66$ mrad and $\phi = 43^\circ$. The inset shows the scheme of the two-layers fitting model.

vectors and the outgoing wave vector \mathbf{Q} . Rotating the sample around the $[001]$ -axis in the total reflection geometry and neglecting the small incidence angle $\theta = 1.66$ mrad, is equivalent to a rotation of the outgoing wave vector in the (001) plane of iron. The position of the outgoing wave vector \mathbf{Q} is defined by the rotation angle ϕ between the $[110]$ direction of iron and \mathbf{Q} (Fig. 1). The delayed intensity decay for various temperatures and the same incidence angle $\theta = 1.66$ mrad is shown in Fig. 2 (inset) together with the angular dependence of the accelerated decay at 1200 K (Fig. 2). Surprisingly the best match to the experimental points was achieved with a 2D square-lattice diffusion model in the (001) iron planes with the jump length equal to a_{Fe} (dashed line). The solid line calculated according to the NN jump diffusion mechanism in bulk bcc α -iron [16]. An other possible jump diffusion mechanism, which we cannot exclude, is a NNN jump diffusion mechanism in a bcc lattice. The reason is the insensitivity of the grazing incidence method to jumps perpendicular to outgoing wave vector \mathbf{Q} , which is nearly parallel to the sample surface (see the phase factor in Eq. (1)).

The diffusion coefficients have been calculated according to the above described model from the accelerated intensity decay measured at various temperatures as presented in the inset of Fig. 2.

The diffusion coefficients in the near-surface 2 nm layer are shown in an Arrhenius plot of Fig. 3 in comparison with bulk diffusion coefficients from different tracer measurements [20]. The diffusion in the near-surface layer is almost two orders of magnitude faster than that in the bulk material and the activation energy determined from the slope of the Arrhenius plot is about 450 meV. In bulk iron a phase transformation from α -iron (bcc) to the γ -iron (fcc) phase takes place at 1184 K. At this temperature the change of iron structure causes a drastic decrease of the diffusion coefficient. In our measurements this step is not visible, thus we think that the bcc structure is stabilised by the MgO substrate or Mo impurities.

Acknowledgements

We kindly acknowledge very helpful discussion with L. Deák. This work was financed by the Austrian Fonds zur Förderung der wissenschaftlichen Forschung (FWF), contract no. P-12492-PHY.

References

- [1] G.V. Smirnov, V.G. Kohn, Phys. Rev. B 52 (1995) 3356.
- [2] V.G. Kohn, G.V. Smirnov, Phys. Rev. B 57 (1998) 5788.
- [3] B. Sepiol, A. Meyer, G. Vogl, H. Franz, R. Ruffer, Phys. Rev. B 57 (1998) 10433.
- [4] B. Sepiol, Mater. Res. Symp. Proc. 527 (1998) 147.
- [5] G. Vogl, B. Sepiol, Hyperf. Interact. 123/124 (1999) 595.
- [6] H. Thiess, M. Kaisermayr, B. Sepiol, M. Sladeczek, R. Ruffer, G. Vogl, Phys. Rev. B 64 (2001) 104305.
- [7] R. Röhlberger, Hyperf. Interact. 123/124 (1999) p. 301 and 455.
- [8] A.I. Chumakov, L. Niesen, D.L. Nagy, E.E. Alp, Hyperf. Interact. 123/124 (1999) 427.
- [9] D.L. Nagy, L. Bottyán, L. Deák, J. Dekoster, G. Langouche, V.G. Semenov, H. Spiering, E. Szilágyi, in: M. Miglierini, D. Petridis (Eds.), Mössbauer Spectroscopy in Materials Science, Kluwer Academic Publishers, Dordrecht, 1999, p. 323.
- [10] B. Lengeler, Synchrotronstrahlung in der Festkörperforschung, 18. IFF Ferienkurs, Kernforschungsanlage Jülich GmbH, 1987.
- [11] R. Röhlberger, Hyperf. Interact. 123/124 (1999) 455.
- [12] T. Urano, T. Kanaji, J. Phys. Soc. Jpn. 57 (1988) 3403.

- [13] R. Moons, S. Blässer, J. Dekoster, A. Vantomine, J. De Wachter, G. Langouche, *Thin Solid Films* 324 (1998) 129.
- [14] S.K.S. Ma, F.W. De Wette, *Surf. Sci.* 78 (1978) 598.
- [15] M.I. Haftel, T.D. Andreadis, J.V. Lill, *Phys. Rev. B* 42 (1990) 11540.
- [16] A. Heiming, K.-H. Steinmetz, G. Vogl, Y. Yoshida, *J. Phys. F, Metal Phys.* 18 (1988) 1491.
- [17] J. Korecki, M. Kubik, N. Spiridis, T. Ślęzak, *Acta Phys. Polonica A* 97 (2000) 129.
- [18] R. Ruffer, A.I. Chumakov, *Hyperf. Interact.* 97/98 (1996) 589.
- [19] H. Spiering, L. Deák, L. Bottyán, *Hyperf. Interact.* 125 (2000) 197.
- [20] Landolt Börnstein, New Series III/26.